

# Yang-Baxter integrable models in experiments: from condensed matter to ultracold atoms

Murray T. Batchelor<sup>1,2</sup> and Angela Foerster<sup>3</sup>

<sup>1</sup> Centre for Modern Physics, Chongqing University, Chongqing 400044, China

<sup>2</sup> Department of Theoretical Physics, Research School of Physics and Engineering,  
and Mathematical Sciences Institute, Australian National University, Canberra ACT  
0200, Australia

<sup>3</sup> Instituto de Física da UFRGS, Av. Bento Gonçalves, 9500, Agronomia, Porto  
Alegre - RS - Brazil

E-mail: batchelor@cqu.edu.cn

E-mail: angela@if.ufrgs.br

**Abstract.** The Yang-Baxter equation has long been recognised as the masterkey to integrability, providing the basis for exactly solved models which capture the fundamental physics of a number of realistic classical and quantum systems. In this article we provide an introductory overview of the impact of Yang-Baxter integrable models on experiments in condensed matter physics and ultracold atoms. A number of prominent examples are mentioned, including the hard-hexagon model, the Heisenberg spin chain, the transverse quantum Ising chain, a spin ladder model, the Lieb-Liniger Bose gas, the Gaudin-Yang Fermi gas and the two-site Bose-Hubbard model. The review concludes by pointing to some other recent developments with promise for further progress.

## Contents

<b>1</b>	<b>Introduction</b>	<b>2</b>
<b>2</b>	<b>Yang-Baxter integrable models in condensed matter</b>	<b>3</b>
2.1	Hard hexagon model . . . . .	3
2.2	Heisenberg spin chain . . . . .	4
2.3	Quantum Ising chain with transverse and longitudinal fields . . . . .	5
2.4	Spin ladder model . . . . .	6
<b>3</b>	<b>Yang-Baxter integrable models in ultracold atoms</b>	<b>8</b>
3.1	Lieb-Liniger Bose gas . . . . .	9
3.1.1	Repulsive regime. . . . .	9
3.1.2	Attractive regime. . . . .	10
3.1.3	Excitations. . . . .	10
3.1.4	Interference experiments. . . . .	11

3.2	Gaudin-Yang Fermi gas with polarization . . . . .	12
3.3	Two-site Bose Hubbard model . . . . .	14
<b>4</b>	<b>Concluding remarks and outlook</b>	<b>16</b>
4.1	Few-body systems . . . . .	17
4.2	Systems out of equilibrium . . . . .	18
4.3	Quantum information processing . . . . .	19
4.4	Quantum simulation of the Yang-Baxter equation . . . . .	19
4.5	Artificial spin ice . . . . .	19

## 1. Introduction

The purpose of this review article is to provide an introductory overview of the impact of exactly solved models, more specifically, the impact of Yang-Baxter integrable models, on experiments. The usefulness of areas of study like statistical mechanics and quantum field theory, which were ultimately seen to be deeply related, is that they address fundamental problems involving realistic model systems of interacting states or particles. In addition to elegant exact solutions of key models, the beauty of these subjects is that mathematical methods developed to tackle the problems at hand have flowered in their own right. A striking example is the Yang-Baxter equation, which has inspired and led to remarkable developments in different branches of mathematics. For example, Yang-Baxter integrable models provide explicit realisations of algebraic structures, such as Lie algebras and quantum groups. On the physics side, both Onsager's exact solution of the two-dimensional Ising model and Baxter's exact solution of the eight-vertex model played key roles in the development of the modern theory of phase transitions and critical phenomena. There are several forces at play in these developments. As already alluded to, the models themselves are fundamental and nontrivial. It should thus come as no surprise that they might eventually be realised in hitherto unimagined experimental settings. However, this was not of course the original motivation for much of this work, which has spanned many decades. Rather, the *raison d'être* was explained by Baxter himself in 1982 [1]:

*Basically, I suppose the justification for studying these models is very simple: they are relevant and they can be solved, so why not do so and see what they tell us?*

And the models have told us so much! Exactly solved models of this kind can be found in many areas of physics, such as condensed matter, quantum field theory, the AdS/CFT correspondence in string theory, nuclear physics, atomic and molecular physics and ultracold atoms. Indeed, the Yang-Baxter equation was quite early recognised as the masterkey to integrability.<sup>‡</sup> Obtaining a solution to the Yang-Baxter equation is tantamount to finding an exactly solved model. Here we present some

<sup>‡</sup> For an historical perspective, including the different forms of the Yang-Baxter equation, see, e.g., [2].

prominent, and rather selective, examples of Yang-Baxter integrable models which have been realised in experiments in the areas of condensed matter physics and ultracold atoms. § Other related developments and some future prospects are mentioned in the conclusion.

## 2. Yang-Baxter integrable models in condensed matter

Condensed matter physics has long been the traditional setting in which a range of exactly solved models have been realised in experiments. These include the early experiments related to the two-dimensional Ising model. In this section we discuss the hard hexagon model, the Heisenberg spin chain, the quantum Ising chain with transverse and longitudinal fields, and a spin ladder model.

### 2.1. Hard hexagon model

The hard-hexagon model is a model defined on the triangular lattice, upon which hexagonal tiles are placed such that the tiles do not overlap. Defining  $g(n, N)$  as the number of ways of placing  $n$  hexagons on  $N$  sites, the combinatorial problem is to calculate

$$f(z) = \lim_{n \rightarrow \infty} \left( \frac{1}{N} \ln Z_N \right), \quad (1)$$

with the grand partition function  $Z_N$  defined by

$$Z_N = \sum_{n=0}^{N/3} z^n g(n, N). \quad (2)$$

The variable  $z$  is the fugacity, related to the density of hexagon tiles by  $\rho = \partial f / \partial z$ . There is a transition from a dense solid phase to a low density “fluid” phase at  $z = z_c$ . Baxter [5] obtained the result

$$f(z) \sim |z - z_c|^{2-\alpha}, \quad (3)$$

with critical exponent  $\alpha = \frac{1}{3}$  and critical point  $z_c = \tau^5$ , where  $\tau = (1 + \sqrt{5})/2$ . The remarkable exact solution of this problem featured the Yang-Baxter equation and saw the first appearance of the celebrated Rogers-Ramanujan identities in statistical mechanics. ||

There have been numerous experimental studies of the behaviour of thin films of gases adsorbed on regular crystal surfaces [8]. In particular, the specific heat of single monolayers of helium adsorbed on graphite was measured [9, 10], with the spectacular peak characteristic of a second order phase transition shown in figure 1. In the vicinity of the peak the specific heat is estimated [10] to diverge as

$$C \sim |T - T_c|^{-\alpha}, \quad (4)$$

§ Some of these developments have been highlighted elsewhere recently [3, 4].

|| For a personal account of these developments the reader is referred to [6]. See also [7].

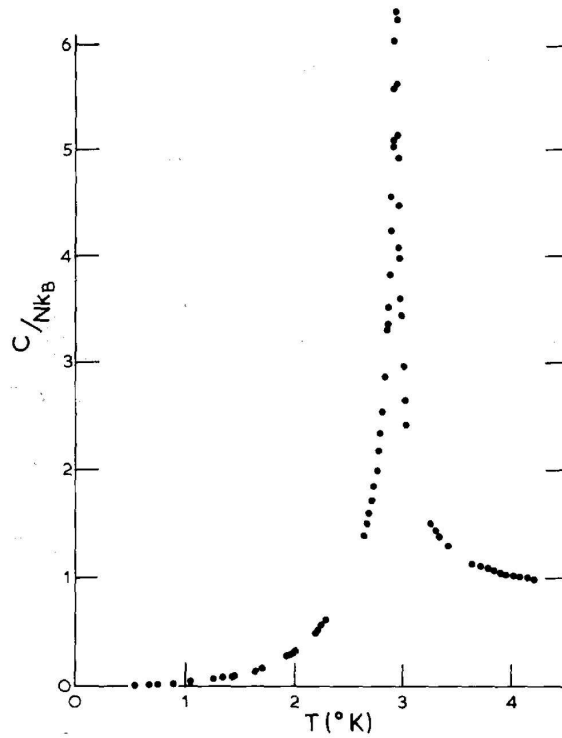


**Figure 1.** Specific heat of helium on graphite at  $\frac{1}{3}$  coverage [9, 10]. Version from [7].

with exponent  $\alpha \approx 0.36$ . The transition observed is from a disordered arrangement of helium atoms at high temperature to an ordered state in which the helium atoms form a regular triangular arrangement. Assuming that the helium atoms can only sit at the centres of the hexagons (which is an approximation) results in a model of a lattice gas on the triangular lattice. The important observation is that the original lattice consists of three sublattices, only one of which can be completely occupied by helium atoms. It was concluded that the transition is in the same universality class as the transition in the 3-state Potts model [11]. In particular, from the equivalence  $z \sim T$  Baxter's exact results for hard hexagons imply also that  $\alpha = \frac{1}{3}$  for the 3-state Potts model. One can thus see that the experimental estimate is rather accurate.

## 2.2. Heisenberg spin chain

The spin- $\frac{1}{2}$  Heisenberg chain [12]

$$\mathcal{H} = J \sum_j \vec{S}_j \cdot \vec{S}_{j+1}, \quad (5)$$

defined in terms of spin- $\frac{1}{2}$  operators  $\vec{S}_j = (S_j^x, S_j^y, S_j^z)$  acting at site  $j$ , is the canonical example of a one-dimensional quantum many-body system solved exactly by means of the Bethe Ansatz [13, 14]. Only much later was it realised that the underlying integrability of the Heisenberg chain is due to the Yang-Baxter equation, governed by the  $R$ -matrix of the related six-vertex model [1, 2, 14].

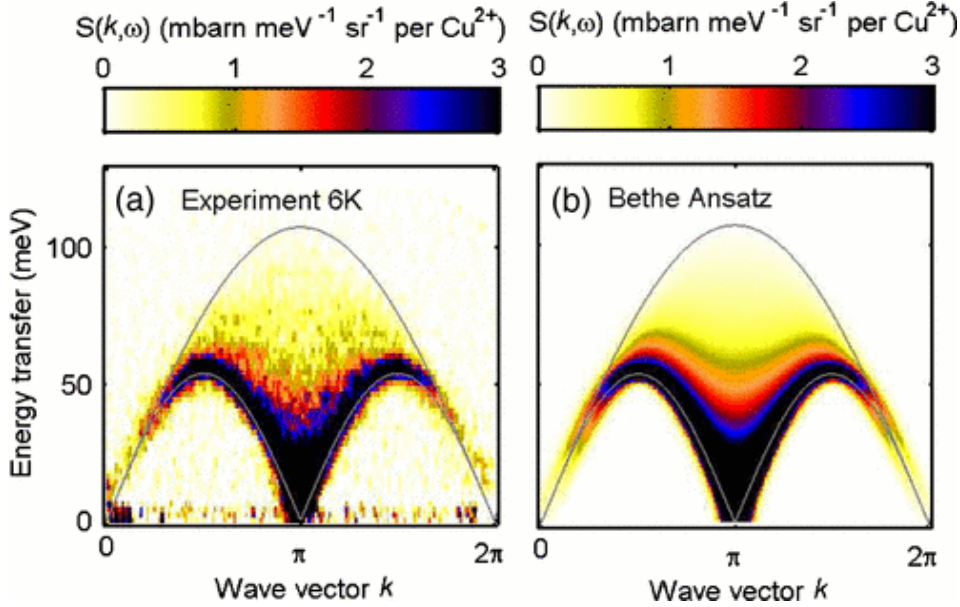


**Figure 2.** Comparison between experiment and theory for the dynamical structure factor of the prototypical Heisenberg antiferromagnetic spin- $\frac{1}{2}$  chain compound  $\text{KCuF}_3$ . (a) Inelastic neutron scattering data from the ISIS Facility, Rutherford Appleton Laboratory, U.K. (b) Theoretical results computed via the algebraic Bethe Ansatz. From [15].

In the compound  $\text{KCuF}_3$  orbital order provides strong Heisenberg coupling between  $\text{Cu}^{2+}$  spin- $\frac{1}{2}$  ions. For energies above a certain threshold, the behaviour of  $\text{KCuF}_3$  is entirely one-dimensional, making it an ideal testbed for the experimental study of the antiferromagnetic spin- $\frac{1}{2}$  Heisenberg chain. The energy and wave vector dependence of the characteristic spinon continuum and the presence of universal scaling behaviour indicating proximity to the Luttinger liquid quantum critical point were established for the first time in  $\text{KCuF}_3$ . Figure 2 shows the direct comparison between the dynamical structure factor obtained from high quality inelastic neutron scattering data for the compound  $\text{KCuF}_3$  and theoretical results obtained via the algebraic Bethe Ansatz for the antiferromagnetic spin- $\frac{1}{2}$  Heisenberg chain [15]. This work also highlighted the inadequacy of conventional approximations in calculating the dynamical structure factor of the antiferromagnetic spin- $\frac{1}{2}$  Heisenberg chain.

The lower and upper boundaries in the multispinon continuum in figure 2(b) are defined by the curves  $\omega_l(k) = \frac{\pi}{2}J|\sin k|$  and  $\omega_u(k) = \pi J|\sin \frac{k}{2}|$ , with  $\omega_l(k)$  describing the dispersion of the basic Faddeev-Takhtajan spinons carrying fractional spin- $\frac{1}{2}$  [16].

### 2.3. Quantum Ising chain with transverse and longitudinal fields

In a state-of-the-art experiment, a quasi-one-dimensional Ising ferromagnet was realised in  $\text{CoNb}_2\text{O}_6$  (cobalt niobate) and tuned through its quantum critical point using strong

transverse magnetic fields [17]. This is the quantum Ising chain with transverse and longitudinal fields – the one-dimensional quantum counterpart of the two-dimensional classical Ising model in a magnetic field – with hamiltonian

$$H = -J \sum_j \left( S_j^z S_{j+1}^z + h S_j^x + h_z S_j^z \right). \quad (6)$$

This model has a quantum critical point at  $h = h_c = J/2$  for  $h_z = 0$ . In the scaling limit sufficiently close to the quantum critical point, i.e.,  $h_z \ll J, h = h_c$ , the spectrum is expected to be described by Zamolodchikov's  $E_8$  mass spectrum [18]. This is the remarkable Yang-Baxter integrable quantum field theory containing eight massive particles with a reflectionless factorized  $S$ -matrix. Up to normalisation, the masses  $m_i$  of these particles coincide with the components of the Perron-Frobenius vector of the Cartan matrix of the Lie algebra  $E_8$ .

The spectrum of this compound was observed by neutron scattering [17], with clear evidence for the first few  $E_8$  masses, see figure 3. The emergence of such an exotic symmetry as  $E_8$  has thus been observed in the lab. We know that the integrable theory provides many more exact predictions [19] than experiments have been able to test so far. Further developments are eagerly awaited on the experimental side.

#### 2.4. Spin ladder model

Many compounds have also been found with effective spin- $\frac{1}{2}$  Heisenberg interactions between spins on a ladder-like structure. The physical properties of such spin ladders are dependent on the number of legs in the ladder. This different behaviour can be seen in figure 4 which shows the measured magnetic susceptibility curves as a function of temperature for the two-leg ladder compound  $\text{SrCu}_2\text{O}_3$  and the three-leg ladder compound  $\text{Sr}_2\text{Cu}_3\text{O}_5$ . In general a spin gap exists in the energy spectrum for even leg ladders while odd leg ladders do not exhibit a gap (see, e.g., [21, 22]).

An integrable spin ladder with two legs was introduced by Yupeng Wang [23] with Hamiltonian

$$\mathcal{H} = \frac{J_{\parallel}}{\gamma} \mathcal{H}_{\text{leg}} + J_{\perp} \sum_{j=1}^L \vec{S}_j \cdot \vec{T}_j - \mu_B g H \sum_{j=1}^L (S_j^z + T_j^z), \quad (7)$$

where

$$\mathcal{H}_{\text{leg}} = \sum_{j=1}^L \left( \vec{S}_j \cdot \vec{S}_{j+1} + \vec{T}_j \cdot \vec{T}_{j+1} + 4(\vec{S}_j \cdot \vec{S}_{j+1})(\vec{T}_j \cdot \vec{T}_{j+1}) \right). \quad (8)$$

Here  $\vec{S}_j$  and  $\vec{T}_j$  are spin- $\frac{1}{2}$  operators acting on sites  $j$  on the left and right legs of the ladder,  $J_{\parallel}$  and  $J_{\perp}$  are the leg and rung couplings,  $\gamma$  is a rescaling constant,  $H$  is the magnetic field and  $L$  is the number of rungs.

This model differs from the usual Heisenberg spin ladder by the presence of the biquadratic interaction terms, which are in essence the price paid to ensure integrability. The model is solved exactly in terms of the Bethe Ansatz: the leg part is simply the permutation operator corresponding to the  $su(4)$  algebra and the rung term becomes

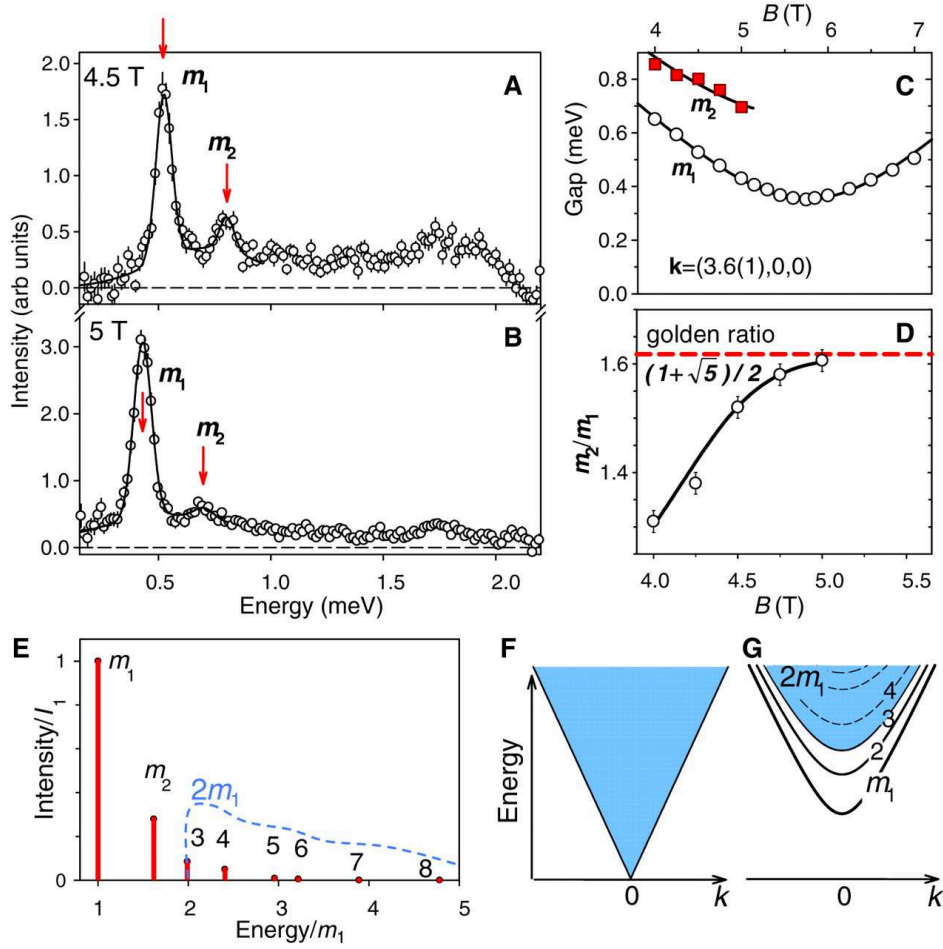


**Figure 3.** Various plots showing experimental evidence for the first few masses of the  $E_8$  mass spectrum in the quasi-1D Ising ferromagnet  $\text{CoNb}_2\text{O}_6$ . From [17].

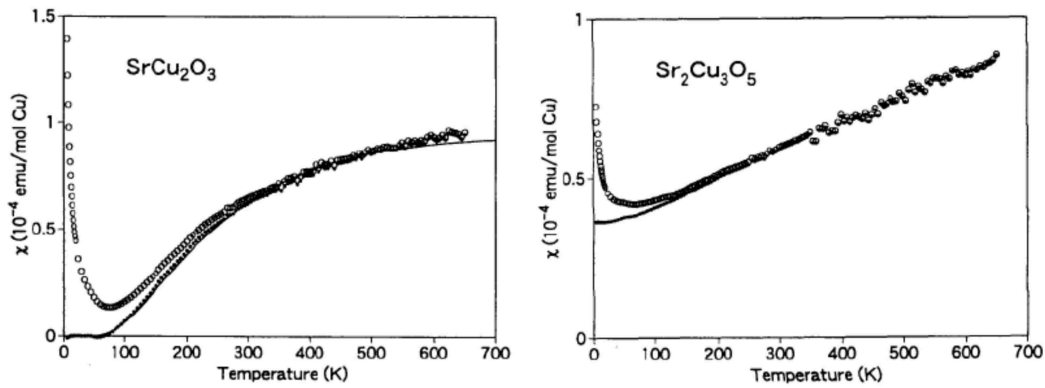


**Figure 4.** Susceptibility versus temperature for (left) the 2-leg ladder compound  $\text{SrCu}_2\text{O}_3$  and (right) the 3-leg ladder compound  $\text{Sr}_2\text{Cu}_3\text{O}_5$ . From [20].

diagonal after a change of basis. The gap and critical fields can be derived using the

Thermodynamic Bethe Ansatz and the thermal and magnetic properties can be obtained using the Quantum Transfer Matrix method [22, 24]. This integrable ladder model can be used to accurately describe the physics of strong coupling ladder compounds, as illustrated in figure 5 for the two-leg ladder compound  $(5\text{IAP})_2\text{CuBr}_4 \cdot 2\text{H}_2\text{O}$ . Similar agreement is seen for other two-leg ladder compounds [22, 24].

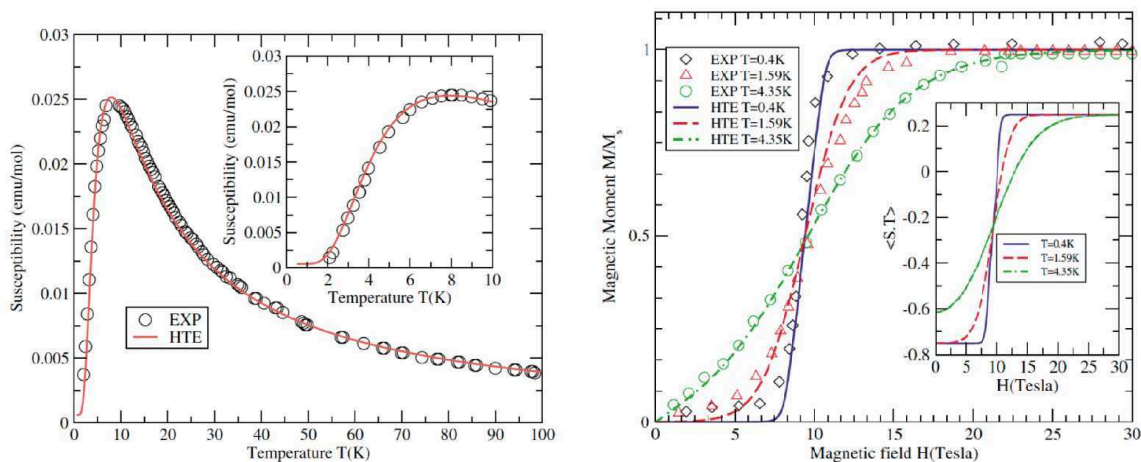


**Figure 5.** Comparison between experiment (EXP) and theory for the two-leg ladder compound  $(5\text{IAP})_2\text{CuBr}_4 \cdot 2\text{H}_2\text{O}$ . (left) Susceptibility versus temperature at  $H = 1\text{T}$  [25]. The solid line denotes the susceptibility evaluated directly from the high temperature expansion (HTE) obtained from the exact solution. A parameter fit suggests the coupling constants  $J_{\perp} = 13.3\text{K}$  and  $J_{\parallel} = 1.15\text{K}$  with  $\gamma = 4$ ,  $g = 2.1$  and  $\mu_B = 0.672\text{K/T}$ . The inset shows the same fit to the susceptibility at low temperature. (right) Magnetisation versus magnetic field [25] with the same constants for different values of the temperature. The inset shows the one-point correlation function versus magnetic field. At  $T = 0.4\text{K}$  the HTE magnetisation curve indicates the critical field values  $H_{c1} \approx 8.3\text{T}$  and  $H_{c2} \approx 10.5\text{T}$ , which are in excellent agreement with the experimental estimates  $8.3\text{T}$  and  $10.4\text{T}$  [25]. From [24].

### 3. Yang-Baxter integrable models in ultracold atoms

The experimental breakthroughs of trapping and cooling atoms to form Bose-Einstein [26] and fermionic [27] condensates led to extraordinary progress in the controlled study of a range of physical phenomena which had not been fully accessible, or at best only partially accessible, through experiments in the more traditional setting of condensed matter physics. Further progress in confining the atoms in tight one-dimensional waveguides, with the ability to vary the interaction strength between atoms, opened up other exciting possibilities. In addition to exploring various aspects of the physics of collective phenomena, the realisation of effectively one-dimensional quantum systems paved the way for contact with some well known exactly solved models. This in turn inspired further theoretical progress. These exciting developments for one-dimensional systems have been reviewed recently [28, 29, 30].



### 3.1. Lieb-Liniger Bose gas

The hamiltonian of  $N$  interacting spinless bosons of mass  $m$  with point interactions on a line of length  $L$  is

$$\mathcal{H} = -\frac{\hbar^2}{2m} \sum_{i=1}^N \frac{\partial^2}{\partial x_i^2} + 2c \sum_{1 \leq i < j \leq N} \delta(x_i - x_j), \quad (9)$$

where  $x_i$  are the boson co-ordinates and  $c$  is the interaction strength. This is the model solved by Lieb and Liniger [31] by means of the Bethe Ansatz wavefunction. The underlying two-body  $S$ -matrix has a scalar form [14, 32]. The Lieb-Liniger model can be obtained in a scaling limit of the spin- $\frac{1}{2}$  XXZ Heisenberg chain (see, e.g., [33]).

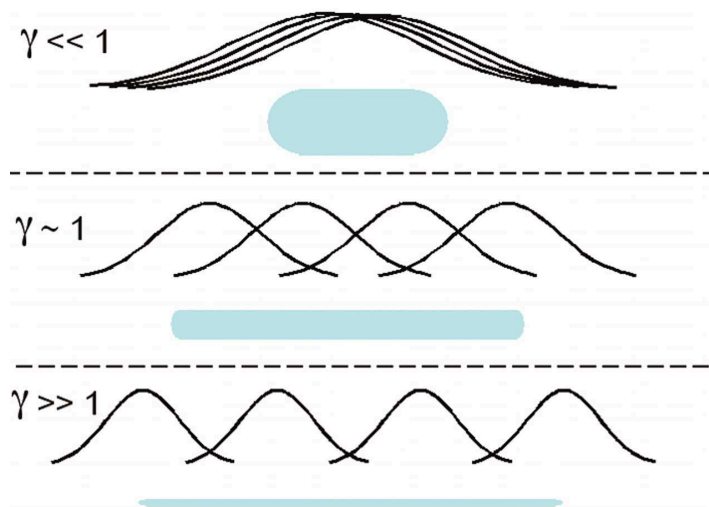


**Figure 6.** Cartoon showing the ‘fermionisation’ of bosons as the interaction strength  $\gamma$  is increased. For  $\gamma \ll 1$  the behaviour is like a condensate, whereas for  $\gamma \gg 1$  the behaviour is like the hard-core bosons of the Tonks-Girardeau gas. From [34].

**3.1.1. Repulsive regime.** In the analysis of the physics of this model it is convenient to define the dimensionless interaction parameter  $\gamma = c/n$  in terms of the number density  $n = N/L$ . A cartoon of the expected atom distributions in the repulsive regime  $c > 0$ , representing the ‘fermionisation’ of the one-dimensional interacting Bose gas with increasing  $\gamma$  is shown in figure 6.

One of the early experiments which made contact with the one-dimensional Lieb-Liniger model of interacting bosons measured local pair correlations in bosonic Rb atoms by photoassociation [35]. The experimental measurement of the local pair correlation function  $g^{(2)}$  is shown in figure 7. This pair correlation function is proportional to the probability of observing two particles in the same location. As expected, the curve drops off towards zero as the interaction strength increases, just like for a non-interacting Fermi gas (recall figure 6).

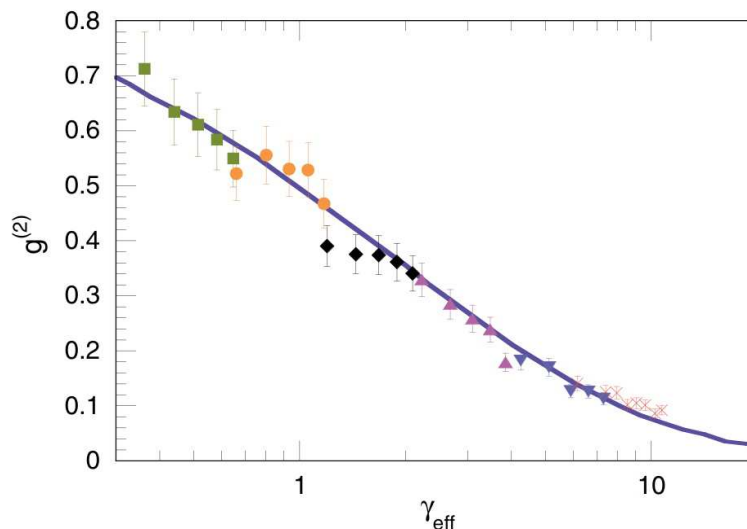


**Figure 7.** Local pair correlation function  $g^{(2)}$  versus effective interaction strength obtained from measuring photoassociation rates in effective one-dimensional tubes of bosonic Rb atoms. The solid line is obtained from the Lieb-Liniger model. From [35].

*3.1.2. Attractive regime.* The attractive regime  $c < 0$  has also been of interest. Inspired by Monte Carlo results which predicted the existence of a super Tonks-Girardeau gas-like state in the attractive interaction regime of quasi-one-dimensional Bose gases [36], it was shown that a super Tonks-Girardeau gas-like state corresponds to a highly-excited Bethe Ansatz state in the integrable Lieb-Liniger Bose gas with attractive interactions, for which the bosons acquire hard-core behaviour [37]. As the interaction is switched from strongly repulsive to strongly attractive the large kinetic energy inherited from the Tonks-Girardeau gas in a Fermi-pressure-like manner prevents the gas from collapsing. Using a tunable quantum gas of bosonic cesium atoms, bosons in the attractive regime were realised and controlled in a one-dimensional geometry to obtain the super Tonks-Girardeau gas [38]. The highly excited quantum phase was stabilised in the presence of attractive interactions by maintaining and strengthening quantum correlations across a confinement-induced resonance (see figure 8). This opened up the experimental study of metastable, excited, many-body phases with strong correlations. In the super Tonks-Girardeau gas relaxation processes are suppressed, making the system metastable over long time scales [39].

*3.1.3. Excitations.* Most recently the excitations of a strongly interacting one-dimensional bosonic quantum gas of  $^{87}\text{Rb}$  atoms have been probed experimentally at low temperature using Bragg spectroscopy and compared to theoretical predictions based on the Lieb-Liniger model for the dynamical structure factor [40]. The excitation spectrum of an ultracold one-dimensional Bose gas of cesium atoms has also been probed experimentally using Bragg spectroscopy [41]. The repulsive contact interactions are

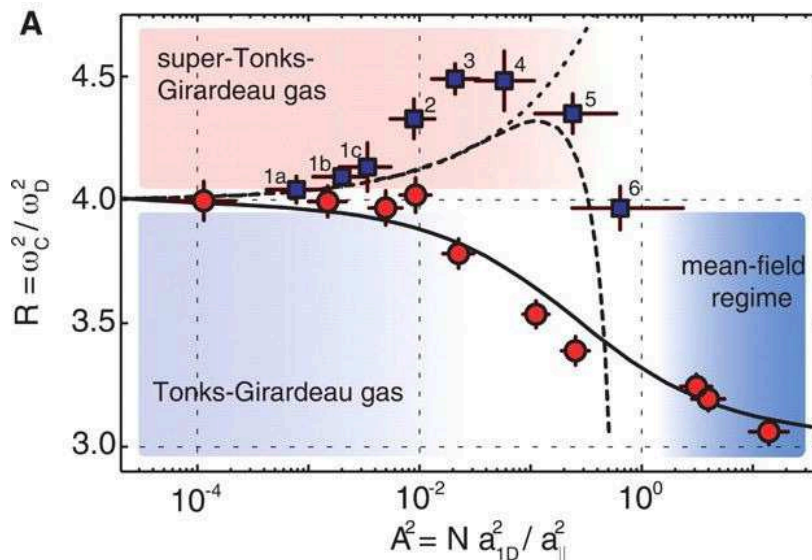


**Figure 8.** Plots of experimental data indicating the realisation of the one-dimensional super Tonks-Girardeau gas with bosonic cesium atoms. From [38].

tuned from the weakly to the strongly interacting regime via a magnetic Feshbach resonance. The measured dynamical structure factor is compared to integrability-based calculations valid at arbitrary interactions and finite temperatures. The results highlight that hole-like excitations, which have no counterpart in higher dimensions and are a distinctive feature of the Bethe Ansatz analysis, actively shape the dynamical response of the gas [41].

It is worth pointing out here in particular that the integrability of the Lieb-Liniger model is actually broken by the presence of the trapping potential along the axis of the one-dimensional gas. In order to compute quantities like the dynamical structure factor of the inhomogeneous trapped gas, the way forward is to use the local density approximation (LDA), where the response of the gas is assumed to be a sum of responses of small portions along the trap with different densities [28, 41, 42]. One then verifies, for example, that the response of the inhomogeneous gas is well approximated by the response of a uniform gas having a density equal to the mean density of the trapped gas. In general the integrable model still drives the underlying physics of the trapped gas.

*3.1.4. Interference experiments.* Yang-Baxter integrability in cold gases has also been used to construct the full distribution function of contrasts for the interference pattern between two independent one-dimensional condensates [43]. In particular, explicit use was made of Baxter’s  $Q$ -operator [1]. The interference-fringe contrast was successfully checked experimentally using two independent one-dimensional quantum degenerate atomic Bose gases of  $\text{Rb}^{87}$  atoms created in a radio-frequency induced micro-trap on an atom chip [44]. In addition to optical lattices, atom chips have provided another platform

for realising one-dimensional Bose gases and various aspects of the Lieb-Liniger model [28, 30].

### 3.2. Gaudin-Yang Fermi gas with polarization

The Hamiltonian

$$\mathcal{H} = -\frac{\hbar^2}{2m} \sum_{i=1}^N \frac{\partial^2}{\partial x_i^2} + g_{1D} \sum_{1 \leq i < j \leq N} \delta(x_i - x_j) - \frac{1}{2} H(N - 2M) \quad (10)$$

describes  $N$  spin- $\frac{1}{2}$  fermions of mass  $m$  interacting via a contact potential on a line of length  $L$  and subject to an external magnetic field  $H$ .  $M$  is the number of spin down fermions, with thus  $N - M$  spin up fermions. The interaction strength  $g_{1D} = \hbar^2 c/m$  can be tuned between the strongly attractive ( $g_{1D} < 0$ ) and strongly repulsive ( $g_{1D} > 0$ ) regimes. Here we consider the attractive regime. This model was solved long ago by Gaudin [45] and Yang [46] in terms of the nested Bethe Ansatz, with a correspondingly more complicated  $S$ -matrix [46, 47, 29]. It received renewed interest in connection with ultracold atomic gases [29, 48].

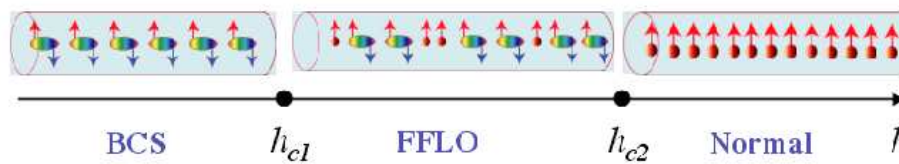


**Figure 9.** The zero temperature phase diagram of the Gaudin-Yang model as a function of magnetic field  $h$  for given chemical potential. The three phases are the fully paired (BCS) phase, which is a quasi-condensate with zero polarization ( $P = 0$ ), the fully polarized (Normal) phase with  $P = 1$ , and the partially polarized (FFLO) phase where  $0 < P < 1$ . The Fulde-Ferrell-Larkin-Ovchinnikov (FFLO) phase is a mixture of pairs and leftover (unpaired) fermions. The quantum critical points  $h_{c1}$  and  $h_{c2}$  separate the FFLO phase from the BCS phase and the normal phase. From [49].

Defining the polarization  $P = (N - 2M)/N$ , the special case  $M = N/2$  for which  $P = 0$  is known as the balanced case. In the attractive regime the roots of the Bethe Ansatz equations tend to form pairs which can be broken by the magnetic field. The quantum critical points distinguishing the different quantum phases (see figure 9) can be calculated (see figure 10) and the full phase diagram mapped out (see figure 11). It is clear that at  $T = 0$  the model predicts three phases in the strong coupling regime: (i) a superfluid phase with zero polarization, where the ground state is composed of pairs; (ii) a fully polarized or ferromagnetic phase with full polarization and (iii) a partially polarized phase, where the ground state is a mixture of pairs and unpolarized fermions.

The phase diagram was confirmed by experiments using fermionic  $^6\text{Li}$  atoms confined to one-dimension [52]. The system has attractive interactions with a spin

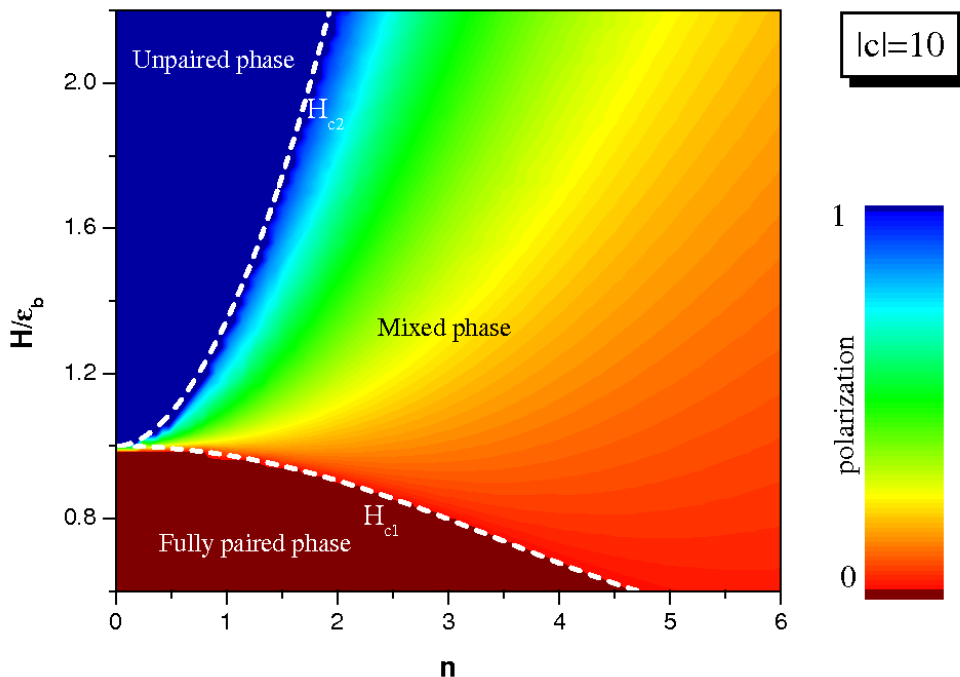


**Figure 10.** Phase diagram of the Gaudin-Yang model for strong coupling  $|c| = 10$  in the  $H - n$  plane, where  $H$  is the external magnetic field and  $n = N/L$  is the linear density. The dashed lines are analytical results for the critical fields obtained from analysis of the dressed energy Thermodynamic Bethe Ansatz equations. These lines are to be compared with the phases (coloured by polarization) obtained from the numerical solution of the dressed energy equations. From [50].

population imbalance caused by a difference in the number of spin-up and spin-down atoms. Experimentally, the gas is dilute and strongly interacting. The key features of the phase diagram (recall figure 11) were experimentally confirmed using finite temperature density profiles (see figure 12). The system has a partially polarized core surrounded by either fully paired or fully polarized wings at low temperatures, in agreement with theoretical predictions [29, 52]. More generally, the experimental results verified the coexistence of pairing and polarization at quantum criticality.

Just as various aspects of the one-dimensional Bose gas have been realised and studied in now over twenty different experiments [28, 30], it is anticipated that various aspects of one-dimensional fermions will be similarly tested and explored in the near future. Recently one-dimensional quantum wires of repulsive fermions with a tunable number of spin components were realised by tightly trapping ultracold  $^{173}\text{Yb}$  atoms in a two-dimensional optical lattice [53]. Optical spin manipulation and detection techniques enabled the system to be prepared in an arbitrary number  $N \leq 6$  of spin components, thus realising different  $\text{SU}(N)$  symmetries. In the study of multi-

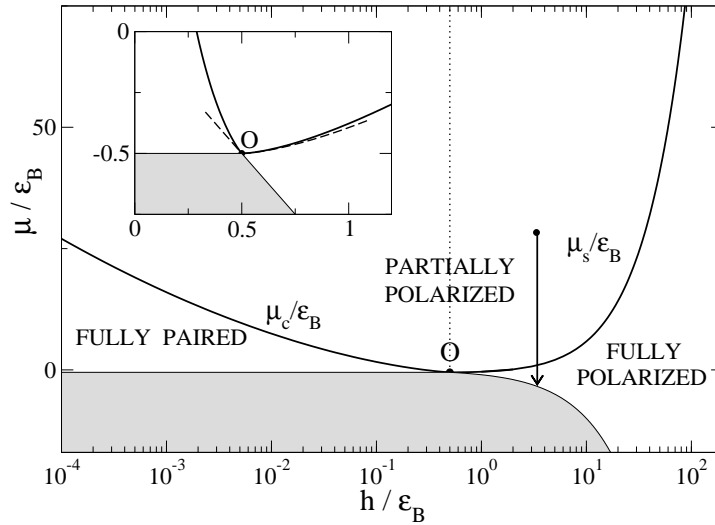


**Figure 11.** Phase diagram of the Gaudin-Yang model as a function of chemical potential and magnetic field. From [51].

component quantum systems Wilson ratios relating magnetic or particle fluctuations to thermal fluctuations have been shown to be particularly powerful dimensionless quantities for probing different magnetic phases in quantum liquids of this kind [54, 55].

### 3.3. Two-site Bose Hubbard model

The two-site Bose-Hubbard model, also known as the canonical Josephson Hamiltonian [56], is a simple model used to study Josephson tunnelling between two Bose-Einstein condensates, whose Hamiltonian is given by

$$H = \frac{1}{8}K(N_1 - N_2)^2 - \frac{1}{2}\Delta\mu(N_1 - N_2) - \frac{1}{2}\mathcal{E}_J(a_1^\dagger a_2 + a_2^\dagger a_1), \quad (11)$$

Despite its apparent simplicity the model captures the essence of competing linear and nonlinear interactions, leading to interesting, nontrivial behaviour. It is not only relevant in the discussion of tunnelling in Bose-Einstein condensates, but also applicable to mesoscopic solid state Josephson junctions [57] and nonlinear optics [58]. Integrable cases of similar models with higher number of modes have been discussed in [59, 60]. Concerning the notation,  $a_1^\dagger, a_2^\dagger$  denote the single-particle creation operators in the two wells and  $N_1 = a_1^\dagger a_1, N_2 = a_2^\dagger a_2$  are the corresponding number operators. The total boson number  $N_1 + N_2$  is conserved and set to the fixed value of  $N$ . The coupling  $K$  provides the strength of the scattering interaction between particles,  $\Delta\mu$  is the external potential and  $\mathcal{E}_J$  is the coupling for the tunnelling.

The model can be exactly solved by the Bethe Ansatz, allowing analytic computation of physical quantities, such as form factors and correlation functions [61] and providing also a characterisation of condensate fragmentation in the attractive

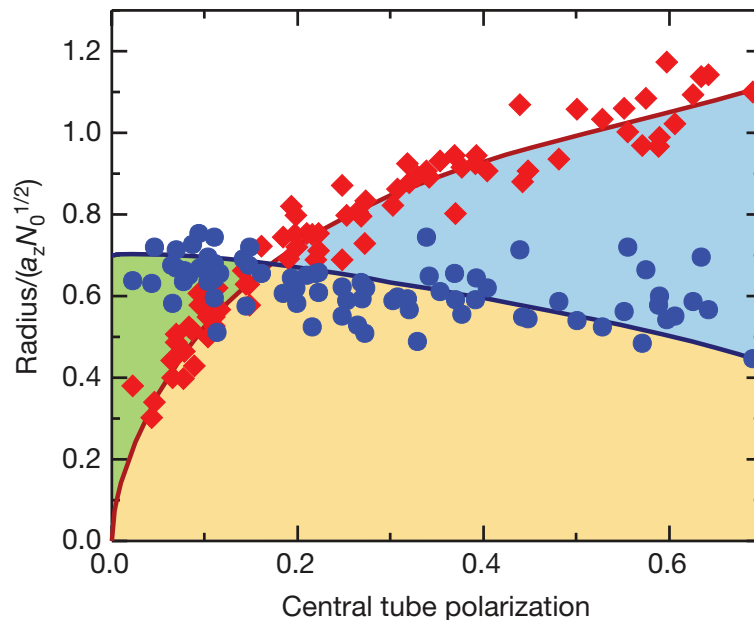


**Figure 12.** Experimental phase diagram of one-dimensional two-component fermions as a function of polarization. The red diamonds and blue circles denote the scaled radii of the axial density difference and the minority state axial density, respectively. The solid lines follow from the Gaudin-Yang model (recall figure 11). From [52].

regime [62]. Although very simple, it describes different relevant physical scenarios, such as tunneling and self-trapping, as can be observed in a study of the quantum dynamics described briefly below. In figure 13 we show the time evolution of the expectation value of the imbalance population  $(N_1 - N_2)/N$  for different ratios of the coupling  $K/\mathcal{E}_J$  and  $\Delta\mu = 0$ . The curves in green (black) are for 100 (400) particles. An initial state is used where all particles are on the left well.

It is clear that the qualitative behaviour does not depend on the precise number of particles. It is interesting to observe in some plots a collapse and revival behaviour, typical of some experiments. In the interval between  $K/\mathcal{E}_J = 1/N$  and  $K/\mathcal{E}_J = 1$  the system tends to localise. In order to see this better, this region is considered in more detail in figure 14. Around  $K/\mathcal{E}_J = 4/N$  there is a threshold in the physical scenario: below this value the amplitude of oscillation of the system runs between positive and negative values, meaning that the particles can tunnel between the two wells, while for values above this threshold the amplitude of oscillation is restricted to positive values, implying that the particles are trapped in one of the wells. Therefore, the quantum dynamics of the two-site Bose Hubbard model describes tunnelling and self-trapping, in qualitative agreement with experiments performed in Oberthaler's group [64].

Recently the model has been also used to describe experiments in ultracold atomic gases on Einstein-Podolsky-Rosen correlations [65] and squeezing [66], relevant in the field of quantum metrology. It can also be used to describe a quadrupolar nuclei system

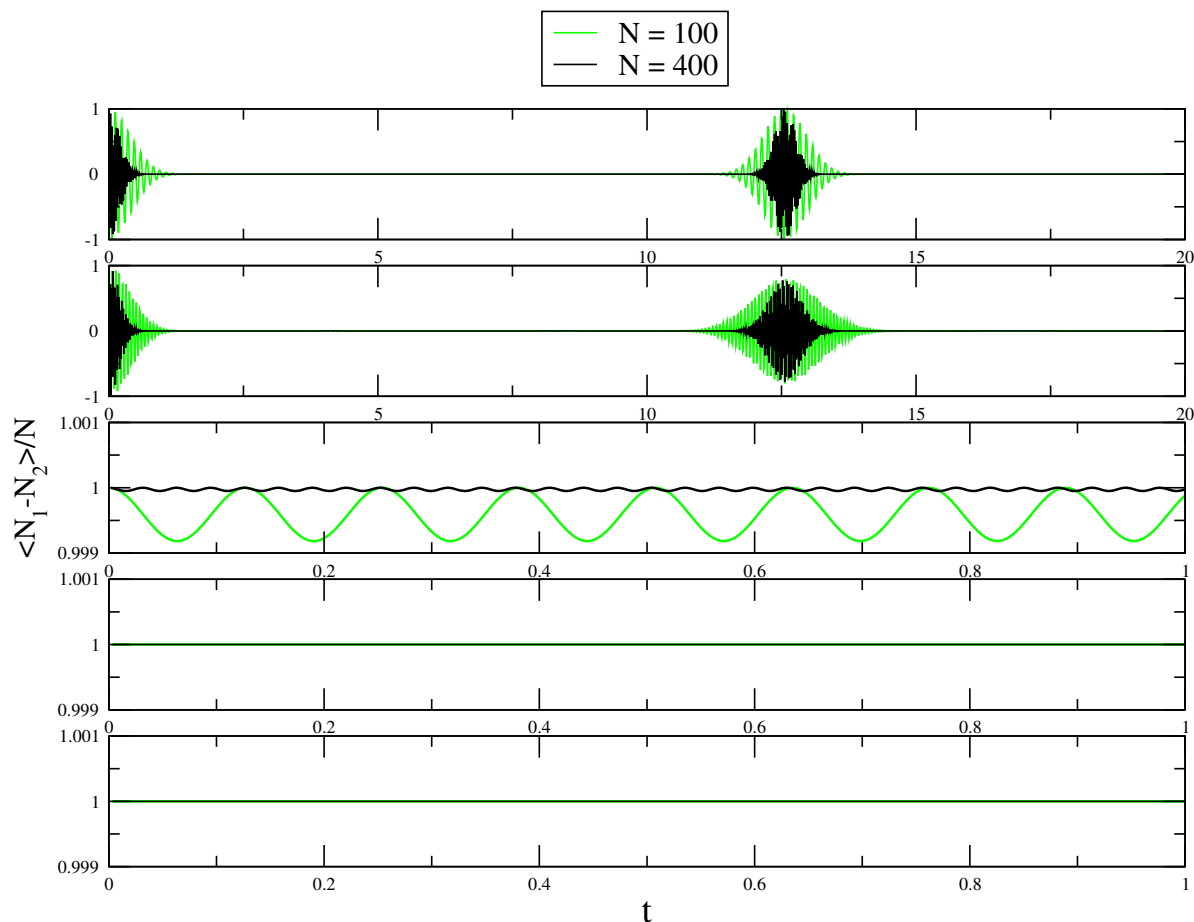


**Figure 13.** Time evolution of the expectation value for the relative number of particles for different ratios of the coupling  $K/\mathcal{E}_J$ . From top to bottom:  $K/\mathcal{E}_J = 1/N^2, 1/N, 1, N, N^2$  for  $N = 100, 400$ . From [63].

in Nuclear Magnetic Resonance (NMR) experiments. In this context, a discussion about protocols of classical bifurcation has been presented in [67] and a novel implementation of spin-squeezed states in NMR, carried out in a liquid crystal sample has been conducted in [68], with possible applications in solid state physics.

#### 4. Concluding remarks and outlook

We have outlined a number of examples in which Yang-Baxter integrable models are relevant to experiments in condensed matter physics and ultracold atoms. This list should be considered remarkable, not necessarily because of the examples given, but arguably also because of what has been omitted. For example, we have not touched on the one-dimensional Hubbard model [69, 70, 71]. Nor did we cover the Anderson model and related quantum dot problems [72]. The discrete BCS model is also an important integrable model in condensed matter, with solutions due to Richardson and Gaudin of relevance to experiments on ultrasmall metallic grains [73]. There are a wealth of exactly



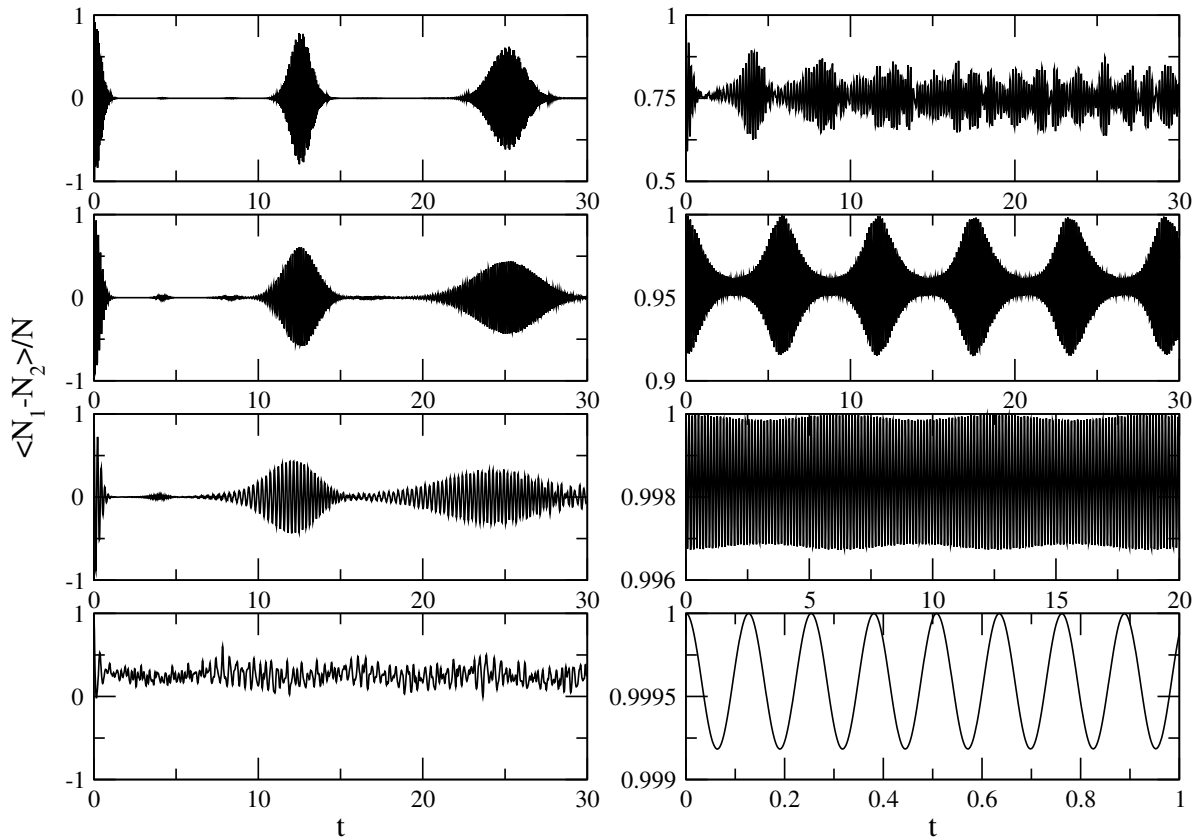


**Figure 14.** Time evolution of the expectation value between  $k/\mathcal{E}_J = 1/N$  and  $k/\mathcal{E}_J = 1$ . On the left, from top to bottom  $k/\mathcal{E}_J = 1/N, 2/N, 3/N, 4/N$  and on the right, from top to bottom  $k/\mathcal{E}_J = 5/N, 10/N, 50/N, 1$ , where  $N = 100$ . From [63].

solved models of this kind which are yet to find their way into experiments.¶ And of course, fundamental work on Yang-Baxter integrable models continues in earnest, with a tremendous amount of knowledge accumulated, for example, on correlation functions. Most recently there has been considerable progress on solving open spin chains with generic integrable boundaries [76, 77]. It is clear that Yang-Baxter integrable models will continue to offer valuable insights into the description of physical properties and experimental results for decades to come. In the remainder of this section we present some other relevant themes, providing an outlook for future research.

#### 4.1. Few-body systems

Despite their simplicity and importance, the investigation of few-body systems has been challenging [78]. Further refinement of experimental techniques in cold atoms have allowed the preparation of few-body ensembles of bosons [79] and fermions [80, 81] in a one-dimensional harmonic trap. The experimental realisation of the McGuire impurity

¶ One only has to glance, for example, through the reprint volume [74] to see just how rich this field is. In addition there are interesting families of quantum chains associated with face models which are yet to be fully explored [75].

model [82] in a one-dimensional Fermi gas has also been reported, where the effects of an impurity are measured by increasing the number of fermions in the system one by one [83]. Other few-particle systems such as the antiferromagnetic Heisenberg spin chain of up to four atoms in a one-dimensional trap have also been experimentally realised, allowing the investigation of quantum magnetism in the ultracold few-body context [84].<sup>+</sup>

These exciting experimental advances stimulated the search for new theoretical methods in few-body systems and also intensified the debate on the nature of the crossover from few to many-body physics. Recent work in this area [87] is inspired by questions like *When is it appropriate to consider a system to be few-body?* and *When should we think of a system as a true many-body system?* In some cases even if a few-body system is not exactly solved by the Bethe Ansatz, some inspiration can still be obtained from these methods. This has been explored, for instance, in [88, 89] where although there is no analytical solution in general, the Bethe Ansatz method has been combined with the variational principle to obtain physical quantities, in agreement with existing results. With the prospect of new few-body experiments in mind, alternative approaches based on the use of the Bethe Ansatz solution are welcome.

#### 4.2. Systems out of equilibrium

The study of quantum systems out of equilibrium is one of the most active frontiers of modern physics. The remarkable experimental realisation of a quantum Newton cradle [90] showing that a one-dimensional Bose gas of  $^{87}\text{Rb}$  does not thermalise after thousands of collisions generated many discussions in the subject of integrability versus quantum thermalisation. Subsequently there has been intense activity in the study of the quantum dynamics of integrable systems, in particular the behaviour of the prototypical Lieb-Liniger model after a quench [91, 92] and a generalised Gibbs ensemble (GGE) has been proposed [93] and improved. A further contribution in this context was given in [94, 95] with the development of the generalised Thermodynamic Bethe Ansatz (GTBA) approach to nonequilibrium evolution, allowing for the computation of local observables at late times after the quench, with impressive reduction in computational complexity as compared to previous approaches. A fundamental issue is the identification of a complete set of the conserved charges, allowing the GGE to predict the correct steady state properties. The GGE has been also discussed for other integrable models, such as the spin- $\frac{1}{2}$  Heisenberg XXZ chain [96], where it was shown that the quasi-local conserved charges [97] are crucial for understanding the non-equilibrium dynamics of the system, which generalizes to other integrable models. Also relevant here is the discovery of Yang-Baxter integrability of boundary driven quantum master equations, which has been reviewed recently [98].

<sup>+</sup> There have been several proposals to realise spin systems in the setting of cold atoms, see, e.g., [85, 86]. Their experimental study thus promises to span the divide between condensed matter and ultracold atoms.

The observation of the excitation spectrum of the one-dimensional Bose gas [41] also opens up some new possibilities. It has been suggested that instead of colliding two highly energetic clouds of atoms like in the quantum cradle setting [90], an alternative could be to observe the time evolution and potential equilibration of collective excitations via the relatively low-energy excitations propagating through the system [41]. On a more general note, besides the fundamental and conceptual issues, the open problems in the study of quantum systems out of equilibrium are also of interest to future quantum technologies.

#### *4.3. Quantum information processing*

Another frontier for experimental developments involving Yang-Baxter integrability is the field of quantum information and computation, an interdisciplinary area that employs the fundamental principles of quantum mechanics to information and computer science [99, 100]. It has been established [101, 102] that certain solutions of the Yang-Baxter equation together with local unitary operators form a universal set of quantum gates, following general earlier results [103]. These results have been explored to investigate, for instance, the dynamical evolution of quantum states. More recently, the Yang-Baxter equation has been connected to teleportation-based quantum computation [104], which is an approach to fault tolerant quantum computation in which the universal quantum gate set is protected from noise using the teleportation protocol [105]. The applications and possibilities in this area are thus also high.

#### *4.4. Quantum simulation of the Yang-Baxter equation*

The relevance of Yang-Baxter integrable models in different fields is clear. Beyond realising further Yang-Baxter integrable systems in the laboratory, it is highly desirable to experimentally implement the Yang-Baxter equation itself in some setting. In the optics framework several proposals for simulating the Yang-Baxter equation have been discussed [106] and a first attempt to verify it has been conducted in [107] using linear quantum optical components such as beamsplitters, half-wave plates, quarter-wave plates, etc. An experimental realisation of the Yang-Baxter equation through a Nuclear Magnetic Resonance interferometric setup has been performed on a liquid state Iodotrifluoroethylene sample of molecules containing three qubits [108], establishing an additional striking connection between integrability on the one hand and quantum information processing on the other. This opens up a way to implement quantum entanglement with integrability and certainly deserves to be further investigated.

#### *4.5. Artificial spin ice*

Apart from the hard hexagon model, with which we began this article, all of the examples given have been for essentially one-dimensional quantum systems. Of course, these models have their two-dimensional classical counterparts. So far there have been, for

example, no experiments performed on related two-dimensional vertex models. As a speculative step in this direction, it may be possible to build on recent experimental advances with artificial spin ice. Artificial spin ice systems are two-dimensional systems constructed with nanomagnetic arrays, vortices in nanostructured superconductors, or soft matter systems (see, e.g., [109] and references therein). Square ice has also been recently observed with water locked between two graphene sheets [110]. Artificial spin ice can be simulated on the square and kagome lattices via colloids in double-well traps [109]. In particular, the systems are built such that the familiar ice-rule is obeyed at each vertex of the square lattice. Examination of such artificial spin ice within the context of the Yang-Baxter integrable vertex models may not be entirely outside the realms of possibility.

## Acknowledgments

It is a pleasure to thank our numerous colleagues for inspiration and collaboration over the years which has shaped our understanding and appreciation of Yang-Baxter integrable models. In particular, we mention here Rodney Baxter, Michael Karowski and Xiwen Guan. We thank Fabrizio Dolcini, Vladimir Gritsev, Jon Links and Tomaz Prosen for helpful comments on this article. MTB gratefully acknowledges support from Chongqing University and the 1000 Talents Program of China. AF acknowledges CNPq (Conselho Nacional de Desenvolvimento Científico e Tecnológico) for financial support. This work has also been partially supported by the Australian Research Council through Discovery Projects DP150101294 and DP130102839.

## References

- [1] Baxter R J 1982 *Exactly solved models in statistical mechanics* (Academic Press, London)
- [2] Au-Yang H and Perk J H H 1989 in *Advanced Studies in Pure Mathematics: Proc. Taniguchi Symp. (Kyoto, Oct. 1988)* (Kinokuniya-Academic, Tokyo) pp 57-94
- [3] Batchelor M T 2014 The importance of being integrable: Out of the paper, into the lab *Int. J. Mod. Phys. B* **28** 1430010
- [4] Guan X W 2014 Critical phenomena in one dimension from a Bethe ansatz perspective *Int. J. Mod. Phys. B* **28** 1430015
- [5] Baxter R J 1980 Hard hexagons: exact solution *J. Phys. A* **13** L61
- [6] Baxter R J 2015 Some academic and personal reminiscences of Rodney James Baxter *J. Phys. A* **48** 254001
- [7] Barber M N 1991 Statistical mechanics: A perspective on the work of R.J. Baxter *Physica A* **170** 221
- [8] Bruch L W, Diehl R D and Venable J A 2007 Progress in the measurement and modeling of physisorbed layers *Rev. Mod. Phys.* **79** 1381
- [9] Bretz M and Dash J G 1971 Ordering transitions in Helium monolayers *Phys. Rev. Lett.* **27** 647
- [10] Bretz M 1977 Ordered helium films on highly uniform graphite – finite size effects, critical parameters, and the three-state Potts model *Phys. Rev. Lett.* **38** 501
- [11] Alexander S 1975 Lattice gas transition of He on Grafoil. A continuous transition with cubic terms *Phys. Lett. A* **54** 353
- [12] Heisenberg W 1928 Zur Theorie des Ferromagnetismus *Z. Phys.* **49** 619

- [13] Bethe H A 1931 Zur Theorie der Metalle. I. Eigenwerte und Eigenfunktionen der linearen Atomkette *Z. Phys.* **71** 205
- [14] Gaudin M 1983 *La fonction d'onde de Bethe* (Masson, Paris)  
Gaudin M 2014 *The Bethe wavefunction* (Cambridge University Press, Cambridge)
- [15] Lake B, Tennant D A, Caux J S, Barthel T, Schollwöck U, Nagler S E and Frost C D 2013 Multispinon continua at zero and finite temperature in a near-ideal Heisenberg chain *Phys. Rev. Lett.* **111** 137205
- [16] Fadeev L D and Takhtajan L A 1981 What is the spin of a spin wave? *Phys. Lett. A* **85** 375
- [17] Coldea R, Tennant D A, Wheeler E M, Wawrzynska E, Prabhakaran D, Telling M, Habicht K, Smeibidl P and Kiefer K 2010 Quantum criticality in an Ising chain: experimental evidence for emergent  $E_8$  symmetry *Science* **327** 177
- [18] Zamolodchikov A B 1989 Integrals of motion and  $S$ -matrix of the (scaled)  $T = T_c$  Ising model with magnetic field *Int. J. Mod. Phys. A* **04** 4235
- [19] Delfino G 2004 Integrable field theory and critical phenomena: the Ising model in a magnetic field *J. Phys. A* **37** R45
- [20] Azuma M, Hiroi Z, Takano M, Ishida K and Kitaoka Y 1994 Observation of a spin gap in  $\text{SrCu}_2\text{O}_3$  comprising spin- $\frac{1}{2}$  quasi-1D two-leg ladders *Phys. Rev. Lett.* **73** 3463
- [21] Dagotto E and Rice T M 1996 Surprises on the way from one- to two-dimensional quantum magnets: the ladder materials *Science* **271** 618  
Dagotto E 1999 Experiments on ladders reveal a complex interplay between a spin-gapped normal state and superconductivity *Rep. Prog. Phys.* **62** 1525
- [22] Batchelor M T, Guan X-W, Oelkers N and Tsuboi Z 2007 Integrable models and quantum spin ladders: comparison between theory and experiment for the strong coupling ladder compounds *Adv. Phys.* **56** 465
- [23] Wang Y 1999 Exact solution of a spin-ladder model *Phys. Rev. B* **60** 9236
- [24] Batchelor M T, Guan X-W, Oelkers N, Sakai K, Tsuboi Z and Foerster A 2003 Exact results for the thermal and magnetic properties of strong coupling ladder compounds *Phys. Rev. Lett.* **91** 217202
- [25] Landee CP, Turnbull MM, Galeriu C, Giantsidis J and Woodward FM 2001 Magnetic properties of a molecular-based spin-ladder system:  $(5\text{IAP})_2\text{CuBr}_4 \cdot 2\text{H}_2\text{O}$  *Phys. Rev. B* **63** 100402(R)
- [26] Anderson M H, Ensher J R, Matthews M R, Wieman C E and Cornell E A 1995 Observation of Bose-Einstein condensation in a dilute atomic vapor *Science* **269** 198  
Davis K B, Mewes M O, Andrews M R, Vandruten M J, Durfee D S, Kurn D M and Ketterle W 1995 Bose-Einstein condensation in a gas of sodium atoms *Phys. Rev. Lett.* **75** 3969
- [27] Greiner M, Regal C A and Jin D S 2003 Emergence of a molecular Bose-Einstein condensate from a Fermi gas *Nature* **426** 537
- [28] Cazalilla M A, Citro R, Giamarchi T, Orignac E and Rigol M 2011 One dimensional bosons: From condensed matter systems to ultracold gases *Rev. Mod. Phys.* **83** 1405
- [29] Guan X W, Batchelor M T and Lee C 2013 Fermi gases in one dimension: From Bethe ansatz to experiments *Rev. Mod. Phys.* **85** 1633
- [30] Jiang Y Z, Chen Y Y and Guan X W 2015 Understanding many-body physics in one dimension from the Lieb-Liniger model *Chin. Phys. B* **24** 050311
- [31] Lieb E H and Liniger W 1963 Exact analysis of an interacting Bose gas. I. General solution and ground state *Phys. Rev.* **130** 1605  
Lieb E H 1963 Exact analysis of an interacting Bose gas. II. Excitation spectrum *Phys. Rev.* **130** 1616
- [32] McGuire J B 1964 Study of exactly soluble one-dimensional  $N$ -body problems *J. Math. Phys.* **5** 662
- [33] Golzer B and Holz A 1987 The nonlinear Schrödinger model as a special continuum limit of the anisotropic Heisenberg model *J. Phys. A* **20** 3327
- [34] Kinoshita T, Wenger T and Weiss D S 2004 Observation of a one-dimensional Tonks-Girardeau

- gas *Science* **305** 1125
- [35] Kinoshita T, Wenger T and Weiss D S 2005 Local pair correlations in one-dimensional Bose gases *Phys. Rev. Lett.* **95** 190406
  - [36] Astrakharchik G E, Boronat J, Casulleras J and Giorgini S 2005 Beyond the Tonks-Girardeau gas: Strongly correlated regime in quasi-one-dimensional Bose gases *Phys. Rev. Lett.* **95** 190407
  - [37] Batchelor M T, Bortz M, Guan X-W and Oelkers N 2005 Evidence for the super Tonks-Girardeau gas *J. Stat. Mech.* L10001
  - [38] Haller E, Gustavsson M, Mark M J, Danzl J G, Hart R, Pupillo G and Nagerl H C 2009 Realization of an excited, strongly correlated quantum gas phase *Science* **325** 1244
  - [39] Panfil M, De Nardis J and Caux J-S 2013 Metastable Criticality and the Super Tonks-Girardeau Gas *Phys. Rev. Lett.* **110** 125302
  - [40] Fabbri N, Panfil M, Clement D, Fallani L, Inguscio M, Fort C and Caux J S 2015 Dynamical structure factor of one-dimensional Bose gases: Experimental signatures of beyond-Luttinger-liquid physics *Phys. Rev. A* **91** 043617
  - [41] Meinert F, Panfil M, Mark M J, Lauber K, Caux J S and Nagerl H C S 2015 Probing the excitations of a Lieb-Liniger gas from weak to strong coupling *Phys. Rev. Lett.* **115** 085301
  - [42] Kheruntsyan K V, Gangardt D M, Drummond P D and Shlyapnikov G V 2005 Finite-temperature correlations and density profiles of an inhomogeneous interacting one-dimensional Bose gas *Phys. Rev. A* **71** 053615
  - [43] Gritsev V, Altman E, Demler E and Polkovnikov A 2006 Full quantum distribution of contrast in interference experiments between interacting one-dimensional Bose liquids *Nat. Phys.* **2** 705
  - [44] Hofferberth S, Lesanovsky I, Schumm T, Imambekov A, Gritsev V, Demler E and Schmiedmayer J 2008 Probing quantum and thermal noise in an interacting many-body system *Nat. Phys.* **4** 489
  - [45] Gaudin M 1967 Un systeme a une dimension de fermions en interaction *Phys. Lett.* **24** 55
  - [46] Yang C N 1967 Some exact results for many-body problem in one dimension with repulsive delta-function interaction *Phys. Rev. Lett.* **19** 1312
  - [47] Sogo K, Uchinami M, Nakamura and Wadati M 1981 Nonrelativistic theory of factorised *S*-matrix *Prog. Theo. Phys.* **66** 1284
  - [48] Batchelor M T, Foerster A, Guan X W and Kuhn C C N 2010 Exactly solvable models and ultracold Fermi gases *J. Stat. Mech.* P12014
  - [49] Zhao E and Liu W V 2010 An effective field theory for one-dimensional polarized Fermi gases *J. Low Temp. Phys.* **158** 36
  - [50] He J S, Foerster A, Guan X W and Batchelor M T 2009 Magnetism and quantum phase transitions in spin-1/2 attractive fermions with polarization *New J. Phys.* **11** 073009
  - [51] Orso G 2007 Attractive Fermi gases with unequal spin populations in highly elongated traps *Phys. Rev. Lett.* **98** 070402
  - [52] Liao Y A, Rittner A S C, Paprotta T, Li W, Partridge G B, Hulet R G, Baur S K and Mueller E J 2010 Spin-imbalance in a one-dimensional Fermi gas *Nature* **467** 567
  - [53] Pagano G, Mancini M, Cappellini G, Lombardi P, Schäfer F, Hu H, Liu X J, Catani J, Sias C, Inguscio M and Fallani L 2014 A one-dimensional liquid of fermions with tunable spin *Nat. Phys.* **10** 198
  - [54] Guan X W, Yin X G, Foerster A, Batchelor M T, Lee C H and Lin H Q 2013 Wilson ratio of Fermi gases in one dimension *Phys. Rev. Lett.* **111** 130401
  - [55] Yu Y C, Chen Y Y, Lin H Q, Römer R A and Guan X W 2015 Dimensionless ratios: characteristics of quantum liquids and their phase transitions arXiv:1508.00763
  - [56] Leggett A J 2001 Bose-Einstein condensation in the alkali gases: Some fundamental concepts *Rev. Mod. Phys.* **73** 307
  - [57] Anglin J R, Drummond P and Smerzi A 2001 Exact quantum phase model for mesoscopic Josephson junctions *Phys. Rev. A* **64** 063605
  - [58] Sanz L, Angelo R M and Furaya K 2003 Entanglement dynamics in a two-mode nonlinear bosonic

- Hamiltonian *J. Phys. A* **36** 9737
- [59] Foerster A and Ragoucy E 2007 Exactly solvable models in atomic and molecular physics *Nucl. Phys. B* **777** 373
  - [60] Tonel A P, Ymai L H, Foerster A and Links J 2015 Integrable model of bosons in a four-well ring with anisotropic tunneling arXiv:1507.07988, accepted for publication in *J. Phys. A*
  - [61] Links J, Zhou H Q, McKenzie R H and Gould M D 2003 Algebraic Bethe ansatz method for the exact calculation of energy spectra and form factors: applications to models of Bose-Einstein condensates and metallic nanograins *J. Phys. A* **36** R63
  - [62] Links J and Marquette I 2015 Ground-state Bethe root densities and quantum phase transitions *J. Phys. A* **48** 045204
  - [63] Tonel A P, Links J and Foerster A 2005 Quantum dynamics of a model for two Josephson-coupled Bose-Einstein condensates *J. Phys. A* **38** 1235
  - [64] Albiez M, Gati R, Fölling J, Hunsmann S, Cristiani M and Oberthaler M K 2005 Quantum dynamics of a model for two Josephson-coupled Bose-Einstein condensates *Phys. Rev. Lett.* **95** 010402
  - [65] Bar-Gill N, Gross C, Kurizki G, Mazets I and Oberthaler M K 2011 Einstein-Podolsky-Rosen correlations of ultracold atomic gases *Phys. Rev. Lett.* **106** 120404
  - [66] Esteve J, Gross C, Weller A, Giovanazzi S and Oberthaler M K 2008 Squeezing and entanglement in a Bose-Einstein condensate *Nature* **455** 1216
  - [67] Araujo-Ferreira A G, Aucaise R, Sarthour R S, Oliveira I S, Bonagamba T J and Roditi I 201 Classical bifurcation in a quadrupolar NMR system *Phys. Rev. A* **87** 053605
  - [68] Aucaise R, Araujo-Ferreira A G, Sarthour R S, Oliveira I S, Bonagamba T J and Roditi I 2015 Spin squeezing in a quadrupolar nuclei NMR system *Phys. Rev. Lett.* **114** 043604
  - [69] Lieb E H and Wu F Y 1968 Absence of Mott transition in an exact solution of short-range one-band model in one dimension *Phys. Rev. Lett.* **20** 1445
  - [70] Essler F H L, Frahm H, Göhmann F, Klümper A and Korepin V E 2005 *The one-dimensional Hubbard model* (Cambridge University Press, Cambridge)
  - [71] Dutta O, Gajda M, Hauke P, Lewenstein M, Lühmann D-S, Malomed B A, Sowinski T and Zakrzewski J 2015 Non-standard Hubbard models in optical lattices: A review *Rep. Prog. Phys.* **78** 066001
  - [72] Konik R M, Saleur R and Ludwig A W W 2001 Transport through quantum dots: Analytic results from integrability *Phys. Rev. Lett.* **87** 236801
  - [73] von Delft J and Ralph D C 2001 Spectroscopy of discrete energy levels in ultrasmall metallic grains *Phys. Rep.* **345** 61
  - [74] Korepin V E and Essler F H L 1994 *Exactly Solvable Models of Strongly Correlated Electrons*, vol. XVIII of Advanced Series in Mathematical Physics (World Scientific, Singapore)
  - [75] Bianchini D, Ercolessi E, Pearce P A and Ravanini F 2015 RSOS quantum chains associated with off-critical minimal models and  $Z_n$  parafermions *J. Stat. Mech.* P03010
  - [76] Kitanine N, Maillet J-M and Niccoli G 2014 Open spin chains with generic integrable boundaries: Baxter equation and Bethe ansatz completeness from SOV *J. Stat. Mech.* P05015
  - [77] Wang Y, Yang W-L, Cao J and Shi K 2015 *Off-diagonal Bethe Ansatz for Exactly Solvable Models* (Springer, Berlin-Heidelberg)
  - [78] Blume D 2012 Few-body physics with ultracold atomic and molecular systems in traps *Rep. Prog. Phys.* **75** 046401
  - [79] Lester B J, Kaufman A M and Regal C A 2014 Raman cooling imaging: Detecting single atoms near their ground state of motion *Phys. Rev. A* **90** 011804(R)
  - [80] Zürn G, Serwane F, Lompe T, Wenz A N, Ries M G, Bohn J E and Jochim S 2012 Fermionization of Two Distinguishable Fermions *Phys. Rev. Lett.* **108** 075303
  - [81] Serwane F, Zürn G, Lompe T, Ottenstein T B, Wenz A N, Jochim S 2011 Deterministic preparation of a tunable few-fermion system *Science* **332** 6027
  - [82] McGuire J B 1965 Interacting fermions in one-dimension. I. Repulsive potential *J. Math. Phys.* **6**

432

- [83] Wenz A N, Zürn G, Murmann S, Brouzos I, Lompe T and Jochim S 2013 From few to many: Observing the formation of a Fermi sea one atom at a time *Science* **342** 6157
- [84] Murmann S, Deuretzbacher F, Zurn G, Bjerlin J, Reimann S M, Santos L, Lompe T and Jochim S 2015 Antiferromagnetic Heisenberg spin chain of few cold atoms in a one-dimensional trap arXiv:1507.01117
- [85] Bloch I, Dalibard J and Nascimbene S 2012 Quantum simulations with ultracold quantum gases *Nature Physics* **8** 267
- [86] Lewenstein M, Sanperra A and Ahufinger V 2012 *Ultracold atoms in optical lattices* (Oxford University Press, Oxford)
- [87] Volosniev A, Fedorov D V, Jensen A S, Valiente M and Zinner N T 2014 Strongly interacting confined quantum systems in one dimension *Nature Comm.* **5** 5300
- [88] Rubeni D, Foerster A and Roditi I 2012 Two interacting fermions in a 1D harmonic trap: matching the Bethe ansatz and variational approaches *Phys. Rev. A* **86** 043619
- [89] Wilson B, Foerster A, Kuhn C C N, Roditi I and Rubeni D 2014 A geometric wave function for few interacting bosons in a harmonic trap *Phys. Lett. A* **378** 1065
- [90] Kinoshita T, Wenger T and Weiss D S 2006 A quantum Newton's cradle *Nature* **440** 900
- [91] Gritsev V, Rostunov T and Demler E 2010 Exact methods in the analysis of the non-equilibrium dynamics of integrable models: application to the study of correlation functions for non-equilibrium 1D Bose gas *J. Stat. Mech.* P05012
- [92] Mossel J and Caux J S 2012 Exact time evolution of space-and time-dependent correlation functions after an interaction quench in the one-dimensional Bose gas *New J. Phys.* **14** 075006
- [93] Rigol M, Dunjko V, Yurovsky V and Olshanii M 2007 Relaxation in a completely integrable many-body quantum system: An ab initio study of the dynamics of the highly excited states of 1D lattice hard-core bosons *Phys. Rev. Lett.* **98** 050405
- [94] Mossel J and Caux J-S 2012 Generalized TBA and generalized Gibbs *J. Phys. A* **45** 255001
- [95] Caux J S and Essler F H L 2013 Time evolution of local observables after quenching to an integrable model *Phys. Rev. Lett.* **110** 257203
- [96] Ilievski E, Nardis J De, Wouters B, Caux J S, Essler F H E and Prosen T 2015 Complete generalized Gibbs ensemble in an interacting theory *Phys. Rev. Lett.* **115** 157201
- [97] Ilievski E, Medenjak M and Prosen T 2015 Quasilocal conserved operators in isotropic Heisenberg spin 1/2 chain *Phys. Rev. Lett.* **115** 120601
- [98] Prosen T 2015 Matrix product solutions of boundary driven quantum chains *J. Phys. A* **48** 373001
- [99] Nielsen M A and Chuang I L 2000 *Quantum Computation and Quantum Information* (Cambridge University Press, Cambridge)
- [100] Li S S, Long G L, Bai F S, Feng S L and Zheng H Z 2001 Quantum computing *Proc. Natl. Acad. Sci. USA* **98** 11847
- [101] Kauffman L H and Lomonaco S J 2004 Braiding operators are universal quantum gates *New J. Phys.* **6** 134
- [102] Zhang Y, Kauffman L H and Ge M L 2005 Universal quantum gate, Yang-Baxterization and hamiltonian *Int. J. Quant. Inform.* **4** 669
- [103] Brylinski J L and Brylinski R 2002 in *Mathematics of Quantum Computation* ed R Brylinski and G Chen (Chapman and Hall/CRC Press, Boca Raton)
- [104] Zhang Y, Zhang K and Pang J 2015 Teleportation-based quantum computation, extended Temperley-Lieb diagrammatical approach and Yang-Baxter equation arXiv:1501.07487
- [105] Gottesman D and Chuang I 1999 Demonstrating the viability of universal quantum computation using teleportation and single-qubit operations *Nature* **402** 390
- [106] Hu S W, Xue K and Ge M L 2008 Optical simulation of the Yang-Baxter equation *Phys. Rev. A* **78** 022319
- [107] Zheng C, Li J L, Song S Y and Long G L 2013 Direct experimental simulation of the Yang-Baxter equation *J. Opt. Soc. Am. B* **30** 1688



- [108] Anvari Vind F, Foerster A, Oliveira I S, Sarthour R S, Soares-Pinto D O, Souza A M and Roditi I 2015 Experimental realization of the Yang-Baxter Equation via NMR interferometry, preprint
- [109] Libál A, Olson Reichhardt C J and Reichhardt C 2015 Doped colloidal artificial spin ice *New J. Phys.* **17** 103010
- [110] Algara-Siller G, Lehtinen O, Wang F C, Nair R R, Kaiser U, Wu H A, Geim A K and Grigorieva I V 2015 Square ice in graphene nanocapillaries *Nature* **519** 443